

1 **Predicting the Stress-Strain Behaviour of Zeolite-Cemented**
2 **Sand based on the Unconfined Compression Test using**
3 **GMDH type Neural Network**

4 Hossein MolaAbasi^{1,*}, Mohammad Saberian², Afshin Kordnaeij³, Jousha Omer⁴, Jie Li⁵ and
5 Parisa Kharazmi⁶

6
7 ^{1,*} Assistant Professor, Department of Civil Engineering, Gonbad University, Gonbad, Iran
8 (Corresponding Author email: hma@gonbad.ac.ir)

9 ² PhD candidate, School of Engineering, RMIT University, Melbourne, Victoria, Australia, E-mail:
10 s3609245@student.rmit.edu.au.

11 ³ PhD candidate, Department of Civil Engineering, Imam Khomeini International University,
12 Ghazvin, Iran

13 ⁴ Senior Lecturer in Civil Engineering, Kingston University, London KT1 2EE, UK

14 ⁵ Associate Professor, School of Engineering, RMIT University, Melbourne, Victoria, Australia,
15 E-mail: jie.li@rmit.edu.au.

16 ³ MSc student, Department of Civil Engineering, Golestan University, Gorgan, Iran

17
18
19
20
21
22
23
24
25
26
27
28

29 **Abstract:**

30 Stabilizing sand with cement is considered to be one of the most cost-effective and useful
31 methods of in-situ soil improvement, and the effectiveness is often assessed using unconfined
32 compressive tests. In certain cases, zeolite and cement blends have been used; however, even
33 though this is a fundamental issue that affects the settlement response of a soil, very few attempts
34 have been made to assess the stress-strain behaviour of the improved soil. Also, the majority of
35 previous studies that predicted the unconfined compressive strength (*UCS*) of zeolite cemented
36 sand did not examine the effect of the soil improvement variables and strain concurrently.
37 Therefore, in this paper, an initiative is taken to predict the relationships for the stress-strain
38 behaviour of cemented and zeolite-cemented sand. The analysis is based on using the unconfined
39 compression test results and Group Method of Data Handling (*GMDH*) type Neural Network
40 (*NN*). To achieve this end, 216 stress-strain diagrams resulting from unconfined compression
41 tests for different cement and zeolite contents, relative densities, and curing times are collected
42 and modelled via *GMDH* type *NN*. In order to increase the accuracy of the predictions, the
43 parameters associated with successive stress and strain increments are considered. The results
44 show that the suggested two and three hidden layer models appropriately characterise the stress-
45 strain variations to produce accurate results. Moreover, the *UCS* values derived from this method
46 are much more accurate than those provided in previous approaches. Moreover, the *UCS* values
47 derived from this method are much more accurate than those provided in previous approaches
48 which simply proposed the *UCS* values based on the content of the chemical binders,
49 compaction, and/or curing time, not considering the relationship between stress and strain.
50 Finally, *GMDH* models can be considered to be a powerful method to determine the mechanical
51 properties of a soil including the stress-strain relationships. The other novelty of the work is that
52 the accuracy of the prediction of the strain-stress behaviour of zeolite-cement-sand samples using
53 the *GMDH* models is much higher than that of the other models.

54

55 **Keywords:** Stabilisation, Zeolite, Cement, Unconfined Compression Test, Stress-Strain
56 Behaviour, *GMDH*.

57

Notation			
R^2	Absolute Fraction of Error	UCS	Unconfined Compressive Strength
$MAPE$	Mean Absolute Error	C	Cement Content
$RMSE$	Root Mean Square Error	Z	Zeolite Replacement Percent
MAD	Mean Absolute Deviation	Dr	Relative Density
M	Total Number of Data	\mathcal{E}	Strain
a_i	Constant Coefficient	q_{n-1}	Stress in the Lower Level
X	Input Vector	day	Curing Time
x_i	Input Variable	$\Delta\mathcal{E}$	Strain Increment
Y	Output Vector	q_{mi}	Measured Stress
y_i	Output Variable	q_{pi}	Predicted Stress

60 1- Introduction

61 With the increasing population of large cities, there is diminishing land space for new
62 construction. Thus, there is an increasing need to build on any existing weak ground by first
63 treating the site soil; for example, saturated loose sand and cement are widely used for this. In
64 some cases, mixing cemented sand with other additives including fibres, glass, or nanoparticles,
65 can make the stabilisation more efficient, especially in pavement construction projects as a
66 support layer for shallow foundations to stabilise and strengthen slopes as well as to prevent sand
67 liquefaction [1].

68 The mechanical and physical properties of cemented sand in different subsections, such as
69 constitutive models, cement blends together with other additives, and the usage of soft
70 computing techniques in predicting the strength properties (e.g., tensile strength (qt) and
71 unconfined compressive strength (UCS)) and stress-strain behaviour have been investigated by
72 several researchers. In this paper, the mechanical behaviour of zeolite-cemented sand is
73 examined (particularly in terms of predicting the stress-strain behaviour obtained from the
74 unconfined compression test) using the Group Method of Data Handling ($GMDH$) type Neural
75 Network (NN). This research aims to propose mathematical models for the stress-strain
76 behaviour of zeolite-cemented sand resulting from unconfined compression tests. Careful

77 consideration is made to accommodate a range of input parameters, such as cement content,
78 zeolite replacement percent, relative density, and curing time.

79 The *GMDH* type *NN* is a combinational multi-layer algorithm that enables progressively
80 improved models to be generated, through the continuous evaluation of performance against a
81 series of multi-input single-output data pairs (X_i, y_i) ($i=1, 2, \dots, M$). *GMDH* was first proposed by
82 Ivakhnenko to determine the functional structure of a model within the empirical data [2].
83 *GMDH* would be applied to model complex systems despite the possibility that there would not
84 be any kind of specific knowledge about them. A model would typically comprise a series (set)
85 of neurons when employing the *GMDH* algorithm so that the different pairs distributed in each
86 layer would be connected by a quadratic polynomial that results in producing new neurons for
87 the next layer. The model would be applied to map inputs to outputs.

88 The majority of previous studies that predicted the *UCS* of zeolite cemented sand did not
89 examine the effect of the soil improvement variables and strain concurrently. Therefore, in the
90 current study, *GMDH*-type *NN* optimised by genetic algorithms are developed to predict the
91 axial stress (q) on the basis of the laboratory test results, which are the characteristics of the
92 zeolite cemented sand properties. Furthermore, in spite of the acceptable performance of
93 computational Intelligence Methods, such as *SVM*, *FIS*, *ANN*, *ANDIS*, and *GEP*, etc., the black-
94 box methods are not completely able to provide practical equations due to their weaknesses as
95 well as their limited applicability and workability [10]. This problem is solved for *GMDH*-type
96 *NN* in this study.

97 In this paper, an initiative is taken to predict relationships for the stress-strain behaviour of
98 cemented and zeolite-cemented sand. Therefore, the *GMDH*-type *NN*, optimised by genetic
99 algorithms, is developed in the current study to estimate and predict the stress-strain of a zeolite
100 cement sand mixture. Finally, the *UCS* values forming the predicted stress-strain diagrams have
101 been compared to previously published empirical correlations.

102

103 **2- Materials and Methods**

104 Cemented sand has been studied by several investigators, mostly in terms of three aspects –
105 proposition of constitutive models based on critical state, cement replacement by additives, and

106 using soft computing techniques to predict the mechanical properties of cemented sand. These
107 aspects are briefly explained in the following sections.

108

109 **2-1- Constitutive Models**

110 In these studies, a constitutive model was proposed to provide the mechanical behaviour of
111 cemented sand. The constitutive model was based on the separation and analysis of the
112 behavioural mechanisms of cemented soils in terms of the distinct responses of the loose soil
113 matrix and the interparticles as two entities. For the uncemented sand, a model was used based
114 on the critical state theory. The model was able to simulate the behaviour of sandy soil in a wide
115 range of confining pressures. An elastic-plastic shear bond model was also employed for the
116 cemented bonds. This combination provided satisfactory results to model the characteristics of
117 the cemented soil in both drained and undrained states. The constitutive model was then
118 validated based on the use of the triaxial test results. The modelling output was a group of
119 deviator axial stress-axial strain, volumetric strain-axial strain, and deviator axial stress-mean
120 effective stress curves [11] and [12].

121

122 **2-2- Mixture of Cement with Other Additives**

123 Some researchers introduced other additives, such as glass, nanoparticles and fibres, into the
124 soils to enhance the strength and reduce the brittleness of the cemented soils [15-18]. Other
125 researchers [17] considered the possibility of the partial replacement of cement by zeolite in the
126 stabilised soils. Zeolite is a natural pozzolan that consists of high amounts of reactive SiO_2 and
127 Al_2O_3 . The oxide components are important in the pozzolanic reactions involved in soil
128 treatment. Table 1 provides some of the previous findings about the addition of zeolite to the
129 cemented sand.

130

131 Table 1. Previous studies on the zeolite-cement-sand blends.

132

133 **2-3- Soft Computing Techniques**

134 Based on the utilisation of the actual soil test results measured in the laboratory, the strength
135 parameters of cemented soils can be expressed by formulating appropriate empirical
136 relationships. To this effect, several empirical correlations based on regression and neural
137 networks have been suggested. Neural networks, being data-driven and of high mathematical/
138 statistical rigour, promise to be superior to regression based empirical correlation, even though
139 the latter are more general in form. In the studies related to regression, Consoli et al. conducted
140 considerable research between 2007 and 2017. In their research, the correlation between the
141 different parameters, such as q_t , and the UCS and triaxial strength to other parameters, including
142 porosity(η) and volumetric cement content (C_v), with the use of an exponential function $a\eta^b c_v^c$ (a,
143 b, and c are constant) were analysed [24] and [25]. Similarly, in 2016, MolaAbasi et al. [21]
144 showed that $\frac{\eta}{C_v}$ is one of the key parameters in the assessment of UCS zeolite cemented sand.

145 There are two approaches to using neural networks in geotechnical applications. In the first
146 approach, the objective is to predict the soil strength properties more accurately than that
147 presently possible with standard regression methods. In the second approach, the aim is to
148 develop stress-strain relationships and behavioural equations, which is the main aim of the
149 current work.

150 Kohestani and Hassanlourad [26] used the artificial neural networks and support vector machine
151 in parallel to study the mechanical behaviour of different types of carbonate sand. The
152 researchers formulated analytical models from an extensive database of triaxial tests performed
153 on three carbonate sand samples. Elsewhere, MolaAbasi and Shooshpasha 2016 suggested a
154 polynomial model for predicting the UCS based on the $GMDH$ that used several input variables,
155 such as cement content, relative density, curing time, and percentage of cement replacement by
156 zeolite. It was observed that cement and zeolite contents strongly influence the UCS [22].

157 Other researchers; namely, Ellis et al. [27], Penumadu and Zhao [28], Zhao et al. [29], and
158 Banimahd et al. [30] used soft computing techniques to model the mechanical behaviour of
159 stabilised soils, but without producing new predictive equations. This kind of limitation is what
160 the present work seeks to overcome for the benefit of engineers designing stabilised soil
161 materials.

162

163 **2-4- Modelling Using the *GMDH* Type Neural Network**

164 The steps of the creation and training processes of the *GMDH* polynomial neural network are
165 summarised as follows [3]:

166

167

168 Figure 1. A graphical example of the *GMDH* training process.

169

170 Step 1: In the first step, the network's first layer is created. Every single neuron is a partial
171 description. The number of neurons is measured by $\frac{n(n-1)}{2}$, where n is the total number of input
172 parameters. Figure 1.1 depicts a layer created for a network with four inputs.

173 Step 2: In this step, the performance evaluation should be done and the neurons providing the
174 poorest results should be removed. Figure 1.2 shows the removed neurons in white (lighter
175 colour).

176 Step 3: Here, one more layer would be created as inputs of the previous layer outputs. The
177 number of neurons for this layer can be also determined by $\frac{n(n-1)}{2}$ (Figure 1.2).

178 Step 4: This stage entails the training and selecting of the neurons on the recently created layer.
179 After the selection, another layer needs to be added (Figure 1.3).

180 Step 5: In this step, training should stop – after the selection process – if any layer includes only
181 one neuron (Figure 1.4).

182 Step 6: The training should be stopped if the best performance value of any layer, except for the
183 first layer, would be poorer than that of the previous layer. In this case, the algorithm adopts the
184 best neuron in the remaining last layer, and deletes the other nodes (Figure 1.5).

185 Step 7: Finally, all the neurons of the previous layers that would not affect the output of the
186 network are removed (Figure 1.6).

187 Recently, genetic algorithms have been considered in a feed forward *GMDH*-type *NN* for each
188 neuron to determine its optimal set of connections with the preceding layer. Recently, *GMDH*-
189 type *NN*, optimised by genetic algorithms, has been considered for different geotechnical
190 applications, such as pile bearing capacity [4], undrained shear strength of clays [5], soil

191 compaction parameters [6], liquefaction potential [7], recompression index [8], compressibility
192 indices of clayey soils [3], and shear strength parameters of marine soils [9].

193

194 **3- Stress-Strain Curve Modelling**

195 In order to model the stress-strain response realistically, a series of unconfined compression test
196 datasets are used. As an illustration, a stress-strain diagram is depicted in Fig. 2 and the variables
197 of the dataset are presented in Table 2. To reserve some of the data for neural network training,
198 considerable effort is made to link the indexes (input parameters) in the model to sample
199 properties. To model GMDH generally, two groups of indexes for each case are selected in the
200 database to include:

- 201 - The features related to the physical properties of the samples; namely, cement content
202 (C), zeolite replacement percent (Z), relative density (D_r), and curing time (t).
- 203 - The features of the soil related to the unconfined compression test; namely,
204 corresponding strain (ϵ), strain increment ($\Delta\epsilon$), and stress in previous strain (q_{n-1}).

205 Additional to the above provisions, the appropriate selection of the stress and strain increments
206 to pair with a previous strain is determined on the basis of neural network training and testing for
207 that particular time series data.

208

209 Figure 2. The stress-strain diagram resulting from unconfined compression tests.

210

211 Table 2. Description of the soil, cement, zeolite, and sample preparations.

212

213 To obtain the stress-strain relationship, an unconfined compression test of two different groups
214 with different input variables are performed.

- 215 - Input parameters of group 1 (*GMDH 1*): including cement content (C), zeolite
216 replacement percent (Z), relative density (D_r), corresponding strain (ϵ), strain increment
217 ($\Delta\epsilon$), and stress in previous strain (q_{n-1}).

218 - Input parameters of group 2 (*GMDH II*): including cement content (C), zeolite
219 replacement percent (Z), relative density (D_r), corresponding strain (ε), strain increment
220 ($\Delta\varepsilon$), stress in previous strain ($qn-1$), and curing time (t).

221 In order to model stress-strain curves, around 80% of the total database is employed for training
222 and the other 20% is used for testing. The number of datasets in *GMDH* modelling of groups 1
223 and 2 are given in Table 3.

224

225 Table 3. The number of datasets in *GMDH* modelling for the training and testing sets.

226

227 Table 4. Statistical parameters of the samples' parameters considered for the *GMDH*.

228

229 One of the fundamental factors to consider in modelling is the optimum percentage of data and
230 the individual sets of values to use for the network training and testing series. For example, if the
231 datasets are randomly dispersed, the model results will be more accurate [8] and [31]. As shown
232 in Table 4, to ensure appropriate selection of the training and testing datasets, the statistical
233 average and variance, as well as the training and testing series, are computed for the whole. As
234 can be seen in Table 4, the statistical variants (the average and variance), training series, testing,
235 and the total data are consistent, showing that the data range is suitable for training and testing.

236

237 **4- Results**

238 Different parameters could be accounted for the *GMDH* prediction process, such as the number
239 of hidden layers, population size, the number of generations, and mutation and crossover
240 probabilities. In optimizing the generalisation performance of the *GMDH* model, the parameter
241 values had to be controlled. In the current study, a population consisting of 100 individuals with
242 mutation and crossover probabilities of 0.01 and 0.95, respectively, was considered in 300
243 generations. As for the hidden layers, the best results were achieved with two and three hidden
244 layers for groups 1 and 2, respectively.

245

246 **4-1- Results of modelling group 1 (GMDH I)**

247 For the first group, a two hidden layer *GMDH* was adopted to estimate and predict the
248 unconfined compressive stresses of the samples cured for 7, 28, and 90 days. The combination of
249 input variables C , Z , D_r , ε , $\Delta\varepsilon$, and q^{n-1} was found to yield the best correlation. Figure 3 provides
250 a view of the structure of the evolved *GMDH*-type *NN*. Eq. (1) shows the polynomials
251 corresponding to this model.

252

$$253 \quad Y_1 = a_1 + a_2 D_r + a_3 \varepsilon + a_4 D_r^2 + a_5 \varepsilon^2 + a_6 D_r \varepsilon \quad (1)$$

$$254 \quad Y_2 = a_1 + a_2 C + a_3 Z + a_4 C^2 + a_5 Z^2 + a_6 CZ$$

$$255 \quad Y_3 = a_1 + a_2 C + a_3 \varepsilon + a_4 C^2 + a_5 \varepsilon^2 + a_6 C \varepsilon$$

$$256 \quad Y_4 = a_1 + a_2 q_{n-1} + a_3 \Delta\varepsilon + a_4 q_{n-1}^2 + a_5 \Delta\varepsilon^2 + a_6 \varepsilon q_{n-1}$$

$$257 \quad Y_5 = a_1 + a_2 Y_1 + a_3 Y_2 + a_4 Y_1^2 + a_5 Y_2^2 + a_6 Y_1 Y_2$$

$$258 \quad Y_6 = a_1 + a_2 Y_3 + a_3 Y_4 + a_4 Y_3^2 + a_5 Y_4^2 + a_6 Y_3 Y_4$$

$$259 \quad q = a_1 + a_2 Y_5 + a_3 Y_6 + a_4 Y_5^2 + a_5 Y_6^2 + a_6 Y_5 Y_6$$

260

261 Where a_i are constant coefficients of Y_1 , Y_2 , Y_3 , Y_4 , Y_5 , and Y_6 ; as presented in Table 5. Fig 4
262 shows the relationship and comparison between the predicted results (from the training) and
263 measured results (from the experimental tests). Based on the figure it can be concluded that the
264 *GMDH* model can be certainly considered for predicting the strength properties.

265

266

Figure 3. A view of the structure of the evolved single hidden layer *GMDH*-type *NN*.

267

268

Table 5. Constant coefficients of Eq. (1).

269 Figure 4. Results obtained from the trained GMDH I with two hidden layers (curing time = 7, 28, and 90).

270

271 **4-2- Results of modelling Group 2 (GMDH II)**

272 For this group, the use of *GMDH* with a three hidden layer neuron connection is illustrated; as

273 presented in Figure 5. The combination of C , Z , Dr , ε , $\Delta\varepsilon$, q^{n-1} , and t as input parameters

274 provides the best correlation, corresponding to the following equation:

275

$$276 \quad Y_1 = a_1 + a_2\varepsilon + a_3\Delta\varepsilon + a_4\varepsilon^2 + a_5\Delta\varepsilon^2 + a_6\varepsilon\Delta\varepsilon \quad (2)$$

$$277 \quad Y_2 = a_1 + a_2\varepsilon + a_3q_{n-1} + a_4\varepsilon^2 + a_5q_{n-1}^2 + a_6\varepsilon q_{n-1}$$

$$278 \quad Y_3 = a_1 + a_2Dr + a_3\Delta\varepsilon + a_4Dr^2 + a_5\Delta\varepsilon^2 + a_6Dr\Delta\varepsilon$$

$$279 \quad Y_4 = a_1 + a_2Z + a_3q_{n-1} + a_4Z^2 + a_5q_{n-1}^2 + a_6Zq_{n-1}$$

$$280 \quad Y_5 = a_1 + a_2C + a_3day + a_4C^2 + a_5ady^2 + a_6Cday$$

$$281 \quad Y_6 = a_1 + a_2Z + a_3Dr + a_4Z^2 + a_5Dr^2 + a_6ZDr$$

$$282 \quad Y_7 = a_1 + a_2Y_1 + a_3\Delta\varepsilon + a_4Y_1^2 + a_5\Delta\varepsilon^2 + a_6Y_1\Delta\varepsilon$$

$$283 \quad Y_8 = a_1 + a_2\Delta\varepsilon + a_3Y_2 + a_4\Delta\varepsilon^2 + a_5Y_2^2 + a_6Y_2\Delta\varepsilon$$

$$284 \quad Y_9 = a_1 + a_2Y_3 + a_3Y_4 + a_4Y_3^2 + a_5Y_4^2 + a_6Y_3Y_4$$

$$285 \quad Y_{10} = a_1 + a_2Y_5 + a_3Y_6 + a_4Y_5^2 + a_5Y_6^2 + a_6Y_5Y_6$$

$$286 \quad Y_{11} = a_1 + a_2Y_7 + a_3Y_8 + a_4Y_7^2 + a_5Y_8^2 + a_6Y_7Y_8$$

$$287 \quad Y_{12} = a_1 + a_2Y_9 + a_3Y_{10} + a_4Y_9^2 + a_5Y_{10}^2 + a_6Y_9Y_{10}$$

$$288 \quad q = a_1 + a_2Y_{11} + a_3Y_{12} + a_4Y_{11}^2 + a_5Y_{12}^2 + a_6Y_{11}Y_{12}$$

289

290 Here, a_i are constant coefficients, values of which are presented in Table 6. Fig. 6 shows the
 291 relationship between the predicted values (using Eq. (2)) and the output target values. Based on
 292 the figure it can be concluded that the experimental results can be successfully modelled and
 293 predicted using the proposed *GMDH* model.

294

295

296 Figure 5. *GMDH II* topology considering curing time.

297

298 Table 6. Constant coefficients of Eq. (2).

299

300 Figure 6. Results obtained from trained *GMDH II* with three hidden layers.

301

302 **4-3- Evaluating *GMDH* type NN Performance**

303 The predictability of the *GMDH* models is shown statistically. The mean absolute percent error
 304 (*MAPE*), mean absolute deviation (*MAD*), root mean squared error (*RMSE*), and absolute
 305 fraction of variance (R^2) have been applied to determine and evaluate the performance of the
 306 *GMDH* models [8].

307

$$308 \quad R^2 = 1 - \left[\frac{\sum_1^M (q_{mi} - q_{pi})^2}{\sum_1^M (q_{mi})^2} \right] \quad (3)$$

$$309 \quad MAPE = \sum_1^M \left| \frac{q_{mi} - q_{pi}}{q_{mi}} \right| \times 100 \quad (4)$$

$$310 \quad RMSE = \sqrt{\frac{1}{M} \sum_1^M (q_{mi} - q_{pi})^2} \quad (5)$$

311
$$MAD = \frac{\sum_1^M |q_{mi} - q_{pi}|}{M}$$
 (6)

312

313 Where q_{mi} and q_{pi} are the measured and predicted values, respectively. The lower the *RMSE*,
314 *MAD*, and *MAPE* values, the better the performance of the *GMDH* models. Based on the results
315 of Table 7, it can be seen that the R^2 values are very close to 1. Therefore, it can be concluded
316 that the performance of the *GMDH* models is acceptable and promising, and that the
317 experimental results can be modelled and predicted using the proposed *GMDH* models.
318 Although the three hidden layer model provides the best results, the double hidden layer model is
319 the most generalised and simplest model.

320

321 Table 7. The performance of the *GMDH* models based on different statistical evaluations.

322

323

324 The application of equations 1 and 2 and resulting plots of the stress-strain curves are explained
325 as follows (see Figure 7):

326 First, stress (q_0) is considered to be zero when the strain is zero ($\epsilon_0 = 0$). Next, having the strain
327 increment ($\Delta\epsilon$) and other input variables, such as stress at previous level (q_0), the stress at the
328 current point can be calculated. On completing this process, the stress-strain curve can be drawn.

329

330

331 Figure 7. The way of plotting the stress-strain diagram or using equations 1 and 2.

332

333 One of the uses of equations 1 and 2 is to determine an appropriate relationship for the strain-
334 stress behaviour of both the cement-only and the zeolite-cement samples, without the need for
335 unconfined compression tests. Hence, based on *GMDH* types 1 and 2, the stress-strain diagrams
336 can be drawn. For instance, the stress-strain behaviour of the 90-day cured sample (C=8% and
337 Dr=85%) has been presented in Figure 8. As clearly evident in Figure 8, *GMDH* types 1 and 2
338 can predict the stress-strain behaviour accurately.

339

340

341 Figure 8. Stress-strain relation for the 90-day sample with 8% cement content and 85% relative density
342 (with the prediction of *GMDH* I, II).

343

344 **5- Discussion**

345 The geotechnical properties of stabilised soils can be estimated using analytical models. Several
346 analytical models have been proposed for cemented sand based on the regression and neural
347 networks. The neural networks approach is more accurate than the regression approach although
348 the regression method is widely adopted since it is less complicated. The neural networks are
349 considered to be powerful tools that come from our current knowledge about the neural networks
350 of animals. Neural networks aim at finding the performance of an issue by using many simple
351 computational elements that relate together with a huge number of connections. *GMDH*-type *NN*
352 is one of the types of neural networks. Compared to the other neural network methods, the
353 *GMDH* method has some advantages in that it (1) provides specific relations for the data, and (2)
354 uses a genetic algorithm for optimisation for finding the neurons and constant coefficients of the
355 model.

356 In order to model the strain-stress behaviour of the UCS test results, several input variables, such
357 as strain increment and stress in previous strain, obtained from the *NN* model have been adopted.
358 Based on the quantitative evaluation of the performance of the *GMDH*-type 1 (i.e., curing time of
359 7, 28, and 90 days) and *GMDH*-type 2 (with considering the curing period parameter) according
360 to the *MAPE*, *MAD*, and *RMSE* results, it can be stated that the *GMDH*-type *NN* is a powerful
361 tool for modelling and evaluation of the relationship between the stress and strain. One of the
362 main practical benefits of the proposed models for obtaining the relationships between the stress
363 and strain of the zeolite-cemented sand based on the *GMDH*-types 1 and 2 is obtaining the stress-
364 strain curves of the samples without conducting the experimental tests.

365 Equations 1 and 2 are also useful for considering the stress-strain relations from the unconfined
366 compression test and the fact that failure occurs when the stress-strain curve reaches a plateau.
367 Thus, the maximum stress (*UCS*) and its corresponding strain can be estimated. From this
368 analysis, the *UCS* graph is drawn in Figure 9 based on the maximum stress of the stress-strain
369 diagrams obtained. Hence, it can be concluded that this approach is completely suitable to
370 estimate the *UCS*.

371 Figure 9. Unconfined compressive strength with the prediction of *GMDH* I, II.

372
373 Although MolaAbasi et al. have already assessed the *UCS* of the cemented and zeolite-cemented
374 specimens using empirical correlations and *GMDH* [22], in this paper, the capability of the
375 current approach is analysed. In Table 8, the employed method is compared with the predicted
376 unconfined compressive strength, other neural networks, and polynomial models. It can be
377 concluded that this method is considerably more accurate and reliable.

378
379 Table 8. Quantitative comparison of previous proposed relations fitting.

380

381 **6- Conclusions**

382 There is limited information about assessing and predicting the stress-strain behaviour of the
383 cement-zeolite improved soil. To illustrate, the majority of previous studies that predicted the
384 *UCS* of zeolite cemented sand did not examine the effect of the soil improvement variables and
385 strain concurrently. Therefore, in this research, the mechanical behaviour of cemented and
386 zeolite cemented sand, including the stress-strain behaviour resulting from the unconfined
387 compression tests and unconfined compressive strength, were predicted. This was done using
388 *GMDH* neural network analysis, from which the following results were established:

- 389 1) Stress in the lower level as well as the strain increment are important parameters in high-
390 accuracy modelling of stress-strain curves.
- 391 2) The optimum modelling for the data of group 1 and group 2 are two hidden layer and
392 three layer modelling, respectively.
- 393 3) Stress-strain diagrams of other parameters in this study range can be drawn based on the
394 proposed equations.
- 395 4) *GMDH* modelling is a high-accuracy approach to predict the stress-strain behaviour of
396 materials.
- 397 5) Unconfined compressive strength can be estimated based on the assessed stress-strain
398 diagrams.
- 399 6) Estimating the unconfined compressive strength based on the approach in this paper is
400 much more accurate than that of previous studies.

401 Finally, the equations presented in this paper are suggested as optimised equations that are
402 applicable in the scope of this study. It is also suggested to consider soft computing methods.
403 Moreover, the prediction of the triaxial behaviour of zeolite-cemented sand is recommended.

404

405 **Conflict of Interest Statement**

406 The authors of this paper have no conflict of interest.

407

408 **References**

- 409 [1] Mola-Abasi H, Kordtabar B, Kordnaeij A. Parameters controlling strength of zeolite–
410 cement–sand mixture. *Int J Geotech Eng.* 2017;11(1):72–79.
- 411 [2] Ivakhnenko AG. Polynomial theory of complex systems. *IEEE Trans Syst Man Cybern.*
412 1971;1(4):364–378.
- 413 [3] Moayed RZ, Kordnaeij A, Mola-Abasi H. Compressibility indices of saturated clays by
414 group method of data handling and genetic algorithms. *Neural Comput Appl.* 2017;1–14.
- 415 [4] Ardalan H, Eslami A, Nariman-Zadeh N. Piles shaft capacity from CPT and CPTu data by
416 polynomial neural networks and genetic algorithms. *Comput Geotech.* 2009;36(4):616–
417 625.
- 418 [5] Kalantary F, Ardalan H, Nariman-Zadeh N. An investigation on the S_u –N SPT
419 correlation using GMDH type neural networks and genetic algorithms. *Eng Geol.*
420 2009;104(1):144–155.
- 421 [6] Ardakani A, Kordnaeij A. Soil compaction parameters prediction using GMDH-type
422 neural network and genetic algorithm. *Eur J Environ Civ Eng.* 2017:1–14.
- 423 [7] Eslami A, Mola-Abasi H, Shourijeh PT. A polynomial model for predicting liquefaction
424 potential from cone penetration test data. *Sci. Iran Trans A Civ Eng.* 2014; 21(1):44–52.
- 425 [8] Kordnaeij A, Kalantary F, Kordtabar B, Mola-Abasi H. Prediction of recompression index
426 using GMDH-type neural network based on geotechnical soil properties. *Soils Found.*
427 2015;55(6):1335–1345.
- 428 [9] Eslami A, Alimirzaei M, Aflaki E, Molaabasi H. Deltaic soil behavior classification using
429 CPTu records—Proposed approach and applied to fifty-four case histories. *Mar*
430 *Georesources Geotechnol.* 2017;35(1):62–79.
- 431 [10] Mohammadzadeh D, Bazaz JB, Alavi AH. An evolutionary computational approach for
432 formulation of compression index of fine-grained soils. *Eng Appl Artif Intell.*
433 2014;33:58–68.
- 434 [11] Haeri SM, Hamidi A. Constitutive modelling of cemented gravelly sands. *Geomech*
435 *Geoengin An Int J.* 2009;4(2):123–139.

- 436 [12] Amini Y, Hamidi A. Triaxial shear behavior of a cement-treated sand-gravel mixture. *J*
437 *Rock Mech Geotech Eng.*2014;6(5):455–465.
- 438 [13] Kutanaei SS, Choobbasti AJ. Experimental study of combined effects of fibers and
439 nanosilica on mechanical properties of cemented sand. *J Mater Civ Eng.* p. 2016;28(6):1-
440 3.
- 441 [14] Javan MH, Haghshenas SS, Kanafi PR, Zartaj H. Investigating the effect of soil
442 behavioral model on the performance of micro pile system under dynamic loading.
443 *Proceedings of the 4th European Conference of Civil Engineering (ECCIE'13), Antalya,*
444 *Turkey.* 2013:8–10.
- 445 [15] Kutanaei SS, Choobbasti AJ. Triaxial behavior of fiber-reinforced cemented sand. *J Adhes*
446 *Sci Technol.* 2016;30(6):579–593.
- 447 [16] Wu P, Houben LJM, Scarpas A, Egyed CEG, de La Roij R. Stiffness modulus and fatigue
448 properties of cement stabilized sand with use of a synthetic modified-zeolite additive.
449 *2015 Annual Meeting of Transportation Research Board.* 2015.
- 450 [17] Salamatpoor S, Jafarian Y, Hajiannia A. Physical and mechanical properties of sand
451 stabilized by cement and natural zeolite. *The European Physical Journal Plus,*
452 *2018;133(205):1–13.*
- 453 [18] Poon CS, Lam L, Kou SC, Lin ZS. A study on the hydration rate of natural zeolite
454 blended cement pastes. *Constr Build Mater.* 1999;13(8):427–432.
- 455 [19] Canpolat F, Yılmaz K, Köse MM, Sümer M, Yurdusev MA. Use of zeolite, coal bottom
456 ash and fly ash as replacement materials in cement production. *Cem Concr Res.*
457 *2004;34(5):731–735.*
- 458 [20] Yılmaz B, Uçar A, Öteyaka B, Uz V. Properties of zeolitic tuff (clinoptilolite) blended
459 Portland cement. *Build Environ.* 2007;42(11):3808–3815.
- 460 [21] Mola-Abasi H, Shooshpasha I. Influence of zeolite and cement additions on mechanical
461 behavior of sandy soil. *J Rock Mech Geotech Eng.* 2016;8(5):746–752.
- 462 [22] Mola-Abasi H, Shooshpasha I. Polynomial models controlling strength of zeolite-cement-

- 463 sand mixtures. *Sci Iran Trans A Civ Eng.* 2017;24(2):526–536.
- 464 [23] Mola-Abasi H, Kordtabar B, Kordnaeij A. Effect of natural zeolite and cement additive on
465 the strength of sand. *Geotech Geol Eng.* 2016;34(5):1539–1551.
- 466 [24] Consoli NC, Foppa D, Festugato L, Heineck KS, Key parameters for strength control of
467 artificially cemented soils. *J Geotech geoenvironmental Eng.* 2007;133(2):197–205.
- 468 [25] Consoli NC. A method proposed for the assessment of failure envelopes of cemented
469 sandy soils. *Eng Geol.* 2014;169:61–68.
- 470 [26] Kohestani VR, Hassanlourad M, Modeling the mechanical behavior of carbonate sands
471 using artificial neural networks and support vector machines. *Int J Geomech.*
472 2015;16(1):1–9.
- 473 [27] Ellis GW, Yao C, Zhao R, Penumadu D. Stress-strain modeling of sands using artificial
474 neural networks. *J Geotech Eng.* 1995;121(5):429–435.
- 475 [28] Penumadu D, Zhao R. Triaxial compression behavior of sand and gravel using artificial
476 neural networks (ANN). *Comput Geotech.* 1999;24(3):207–230.
- 477 [29] Zhao H, Huang Z, Zou Z. Simulating the stress-strain relationship of geomaterials by
478 support vector machine. *Math Probl Eng.* 2014;2014:1–7.
- 479 [30] Banimahd M, Yasrobi SS, Woodward PK. Artificial neural network for stress–strain
480 behavior of sandy soils: Knowledge based verification. *Comput Geotech.* 2005;32(5):377–
481 386.
- 482 [31] Hassanlourad M, Ardakani A, Kordnaeij A, Mola-Abasi H. Dry unit weight of compacted
483 soils prediction using GMDH-type neural network. *Eur Phys J Plus.* 2017;132(8)1–11.

484

Figure 1

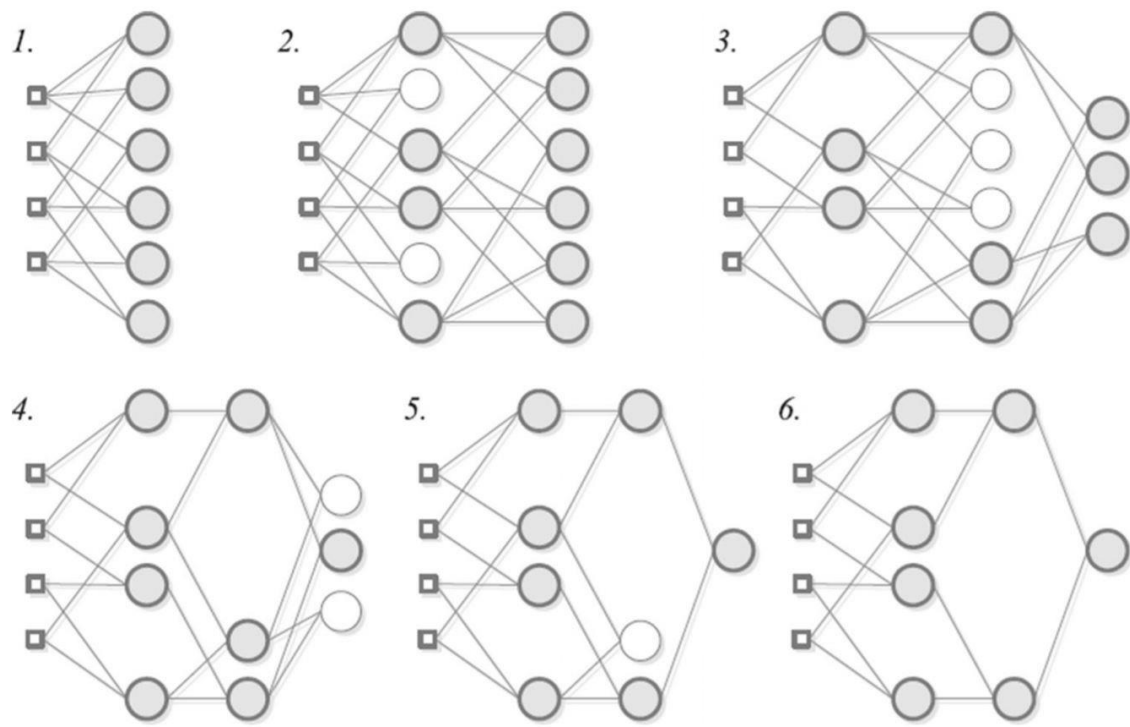


Figure2

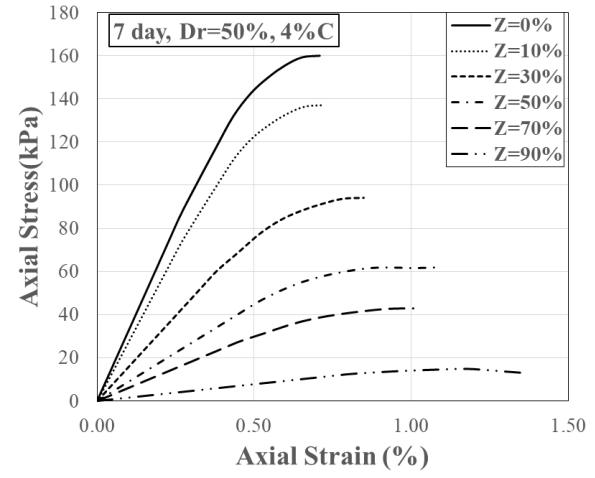
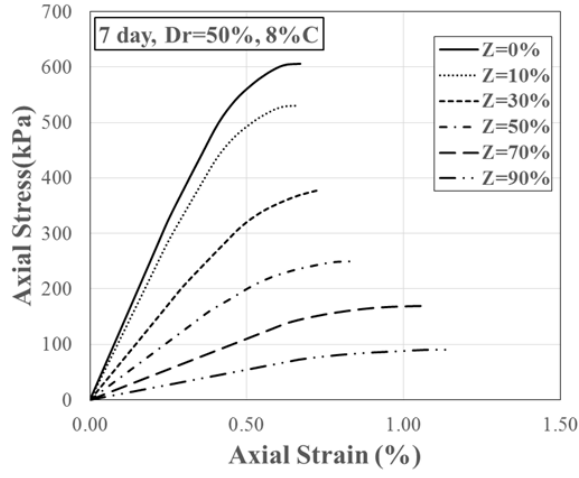


Figure3

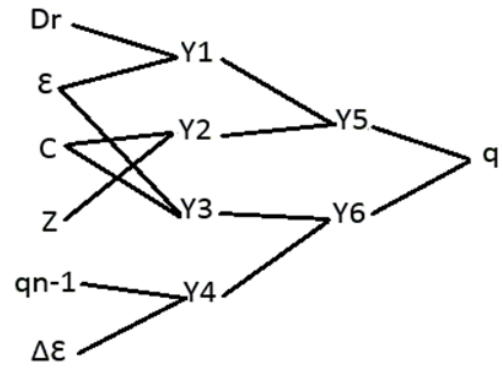


Figure4

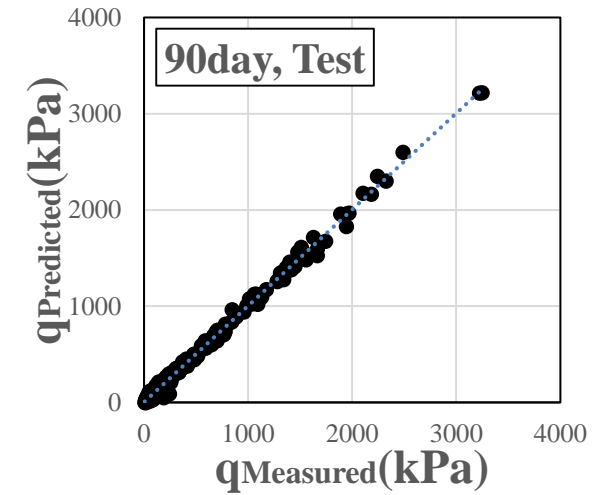
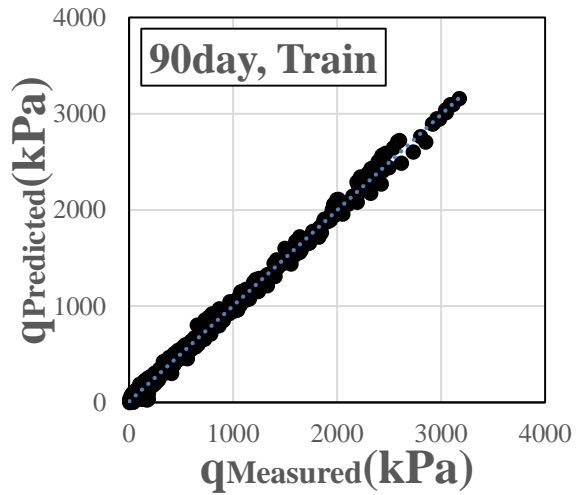
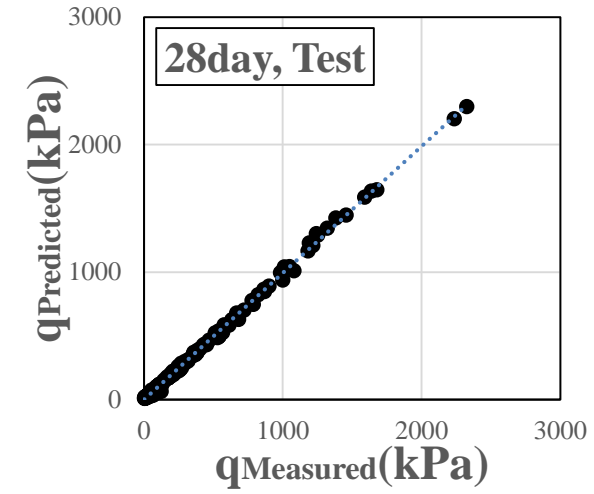
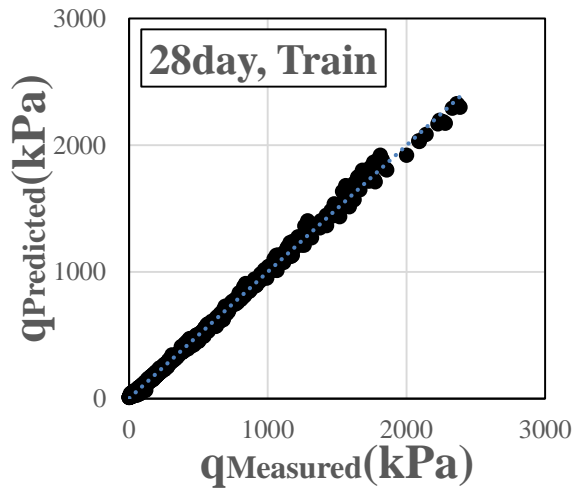
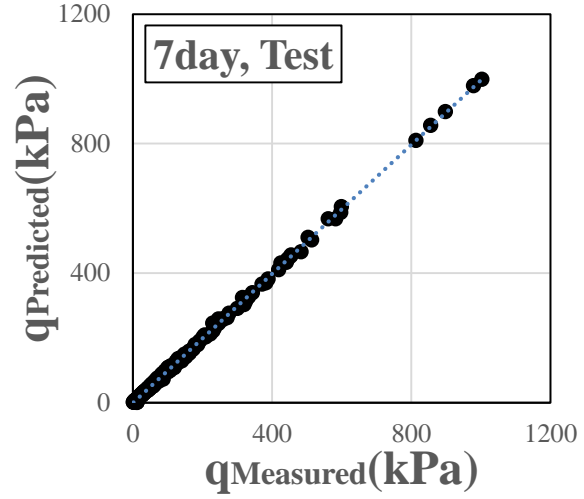
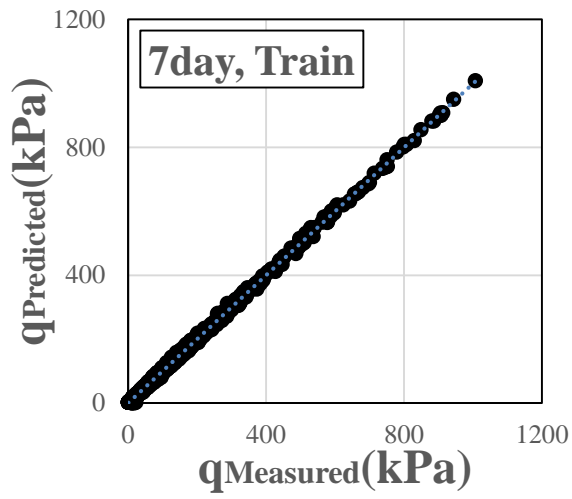


Figure5

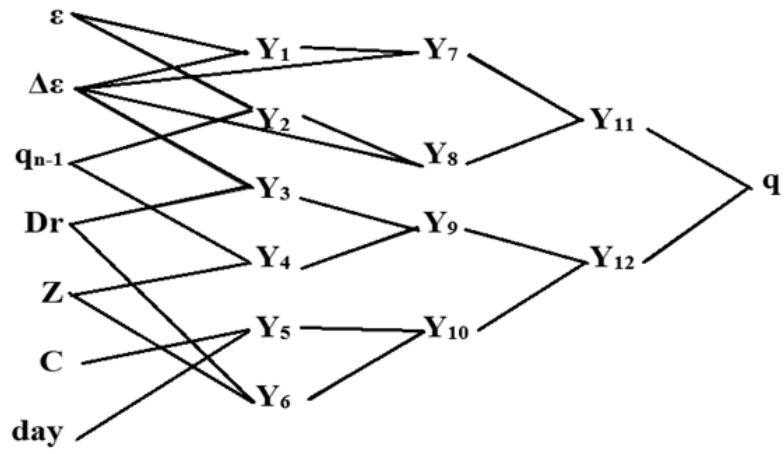


Figure6

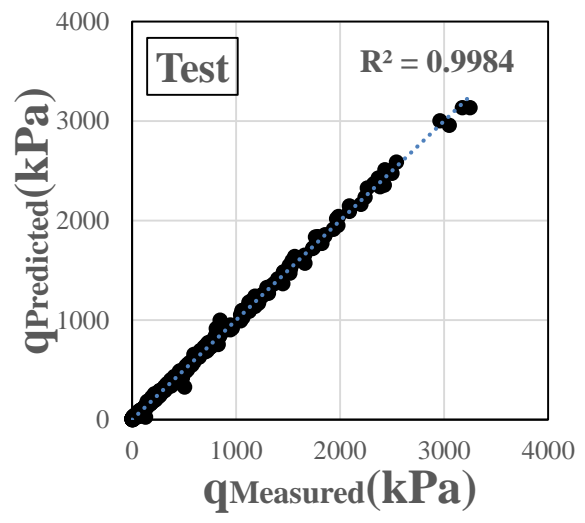
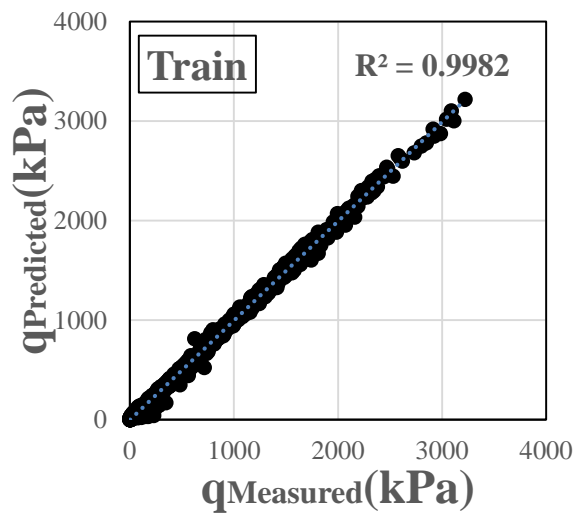


Figure 7

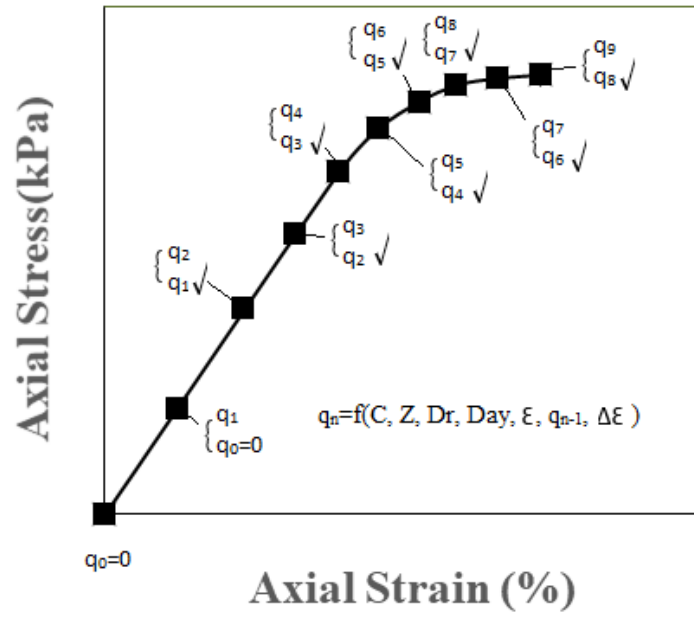


Figure8

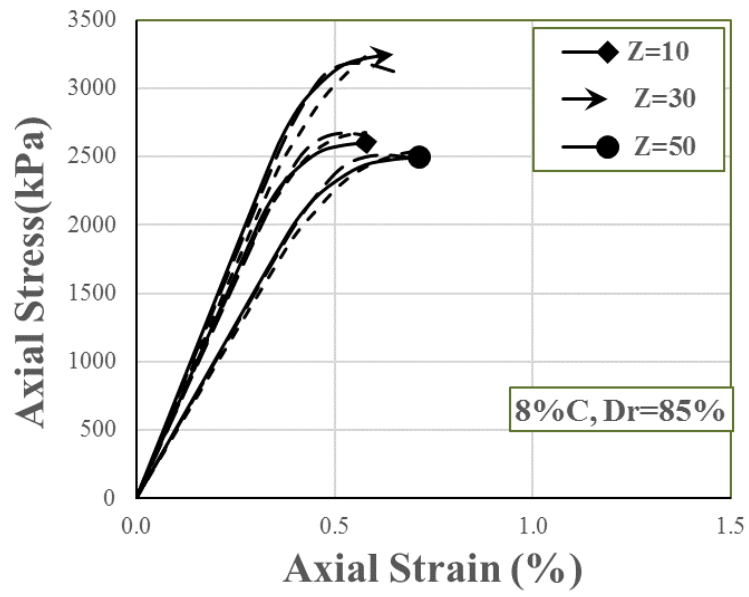
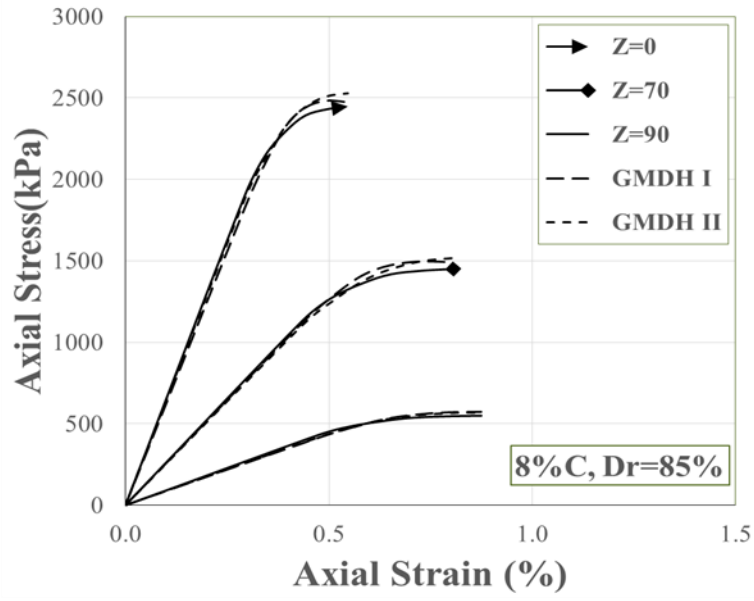
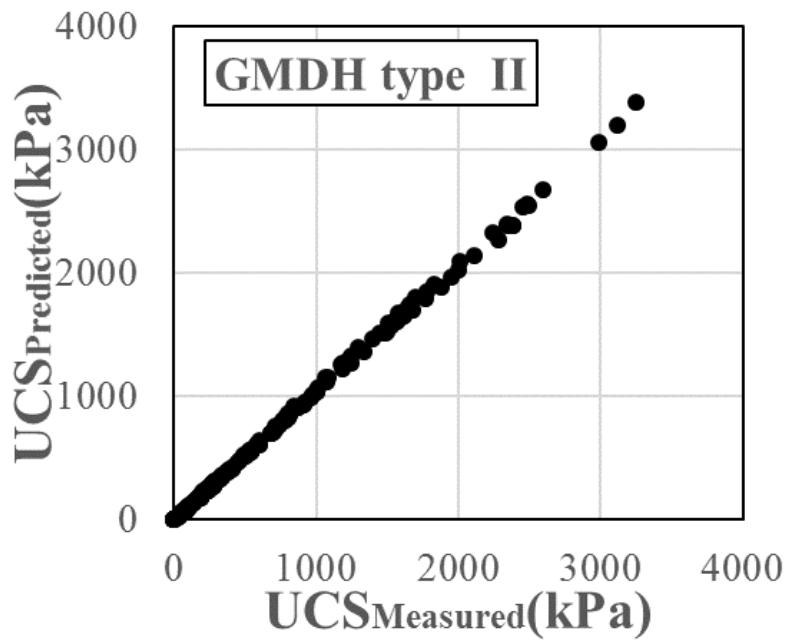
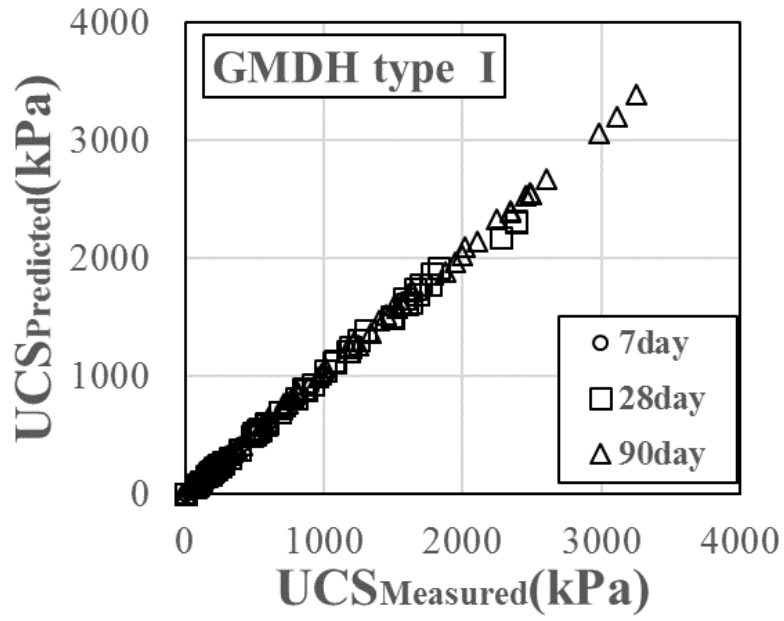


Figure9



No.	Results
1	Addition of zeolite reduced the porosity of the blended cement paste. It also improved the interfacial microstructure properties of the cemented pastes [18].
2	Substitution of zeolite significantly increased the strength of cement because of the pozzolanic reactions with $Ca(OH)_2$. Moreover, the addition of zeolite prevented the undesirable expansion due to alkali-aggregate reactions [19].
3	The addition of a clinoptilolite kind of zeolite reduced the specific gravity of the cemented soil [20].
4	The addition of zeolite to the cement-sand mixtures resulted in increasing the strain rate at failure and the ductility of the samples [21].
5	The replacement of cement by zeolite at 30% led to providing the highest <i>UCS</i> value of the zeolite-cement-sand blends after 28 days of curing [22].
6	Compared to the cemented sand, the zeolite-cement-sand blends provided stronger adsorptive capacity of Chemical Oxygen Demand (<i>COD</i>). In addition, the replacement of cement by natural zeolite resulted in increasing the <i>PH</i> . Also, the addition of zeolite in the cemented sand mixtures improved the microstructure of the blends because of filling more pores as well as providing more pozzolanic reactions [25].
7	It was proposed that the porosity/cement content ratio could be considered to be an acceptable parameter for evaluation of the <i>UCS</i> of zeolite-cemented sand. Also, a unique relationship was presented to relate the <i>UCS</i> to porosity as well as <i>UCS</i> to the zeolite and cement contents [1].

Variable and properties	Descriptions and values
Type of soil	Poorly graded sand (SP)
Type of cement	Type II Portland cement
Cement content	2, 4, 6, and 8% (by dry weight of the soil)
Type of zeolite	Natural clinoptilolite zeolite
Zeolite content	0, 10, 30, 50, 70, and 90% of cement
Void ratio	Related to $D_r = 50, 70,$ and 85% of sand
Water content	10% (by dry weight of the soil)
Size of the samples	76 mm height and 38 mm diameter
Curing periods	7, 28, and 90 days

Set	7 days	28 days	90 days	Total
Training	1186	896	831	2914
Testing	297	225	208	729
Total	1483	1121	1039	3643

Group	Statistical parameters	Set	Stress (kPa)	Curing time (days)	Strain increment (%)	Stress in previous strain (kPa) (q_{n-1})	Corresponding strain (ϵ (%))	Relative density (D_r (%))	Zeolite replacement (Z (%))	Cement content (C (%))
Group 1 GMDHI	Mean	Train	110.81	7	0.06	99.80	0.69	68.12	39.10	5.13
		Test	124.46	7	0.06	112.25	0.76	69.79	39.18	5.07
		Total	112.95	7	0.06	101.75	0.70	68.38	39.12	5.12
	Variance	Train	159.64	7	0.02	150.59	0.43	14.37	30.93	2.21
		Test	171.80	7	0.02	161.09	0.42	14.10	30.92	2.12
		Total	161.62	7	0.02	152.30	0.42	14.33	30.92	2.20
	Mean	Train	398.48	28	0.06	351.30	0.53	68.16	39.12	5.09
		Test	348.00	28	0.06	301.83	0.50	69.41	39.71	5.09
		Total	390.82	28	0.06	343.79	0.53	68.35	39.21	5.09
	Variance	Train	487.68	28	0.01	459.36	0.31	14.32	30.60	2.24
		Test	433.34	28	0.02	409.07	0.33	14.50	30.14	2.24
		Total	479.99	28	0.01	452.26	0.32	14.35	30.52	2.24
	Mean	Train	581.10	90	0.06	510.43	0.54	68.58	39.04	5.09
		Test	492.64	90	0.06	435.94	0.51	69.03	38.59	5.00
		Total	567.18	90	0.06	498.72	0.53	68.66	38.97	5.07
	Variance	Train	666.86	90	0.04	630.16	0.30	14.31	30.17	2.20
		Test	634.61	90	0.03	603.72	0.32	13.99	31.65	2.17
		Total	662.10	90	0.03	626.15	0.30	14.26	30.39	2.19
Group 2 GMDH II	Mean	Train	480.84	34.67	0.06	448.52	0.37	14.35	39.14	5.10
		Test	497.61	34.48	0.06	465.20	0.37	14.31	39.01	5.00
		Total	493.65	34.62	0.06	461.12	0.37	14.31	39.10	5.07
	Variance	Train	480.84	34.67	0.02	448.52	0.37	14.35	30.60	2.22
		Test	497.61	34.48	0.02	465.20	0.37	14.31	30.57	2.20
		Total	493.65	34.62	0.02	461.12	0.37	14.31	30.64	2.15

		a₁	a₂	a₃	a₄	a₅	a₆
7 days	Y₁	2.993316	-13.2598	1.436345	8.709119636	-0.0001	-0.29828
	Y₂/100	0.082905	-0.37509	1.888064	0.036901252	-1.98379	0.495729
	Y₃	-10.282	11.08636	0.687695	4.418622211	0.004183	-0.52284
	Y₄/10000	-0.05414	0.000719	1.29376	-2.8633E-06	-9.7769	-0.00239
	Y₅	0.729246	0.951207	0.010892	-3.1538E-05	-3.9E-05	0.000228
	Y₆	26.24902	-0.26571	-0.0907	0.000102091	-0.00047	0.009367
	q	-0.01297	0.980512	0.012481	-7.4979E-05	-6.7E-05	0.00022
28 days	Y₁/100	0.389613	-1.15843	0.013952	0.791759356	-4.9E-07	-0.0036
	Y₂/100	-1.5907	-0.49019	9.151163	0.095505468	-9.76299	1.637782
	Y₃/100	-2.98565	1.257557	0.132167	0.050231261	-0.00148	-0.01063
	Y₄/100000	-0.022	5.1E-05	0.781469	-8.653E-08	-5.8985	-0.00037
	Y₅	-5.79414	0.954868	0.070322	-6.4801E-06	-5.4E-05	4.83E-05
	Y₆	68.88962	-0.77483	0.28929	0.000315706	-0.00095	0.003281
	q	-2.61946	0.956091	0.025773	-2.1089E-05	2.66E-06	6.09E-05
90 days	Y₁/100	0.673826	-1.52856	0.013239	0.887138827	-2.5E-07	-0.00291
	Y₂/1000	-0.11414	-0.1317	1.525918	0.021511191	-1.56807	0.191593
	Y₃/100	-1.73283	0.277275	0.185731	0.261869734	-0.00191	-0.01846
	Y₄/10000	0.041988	-0.00046	0.5381	3.81725E-06	-2.26203	0.001311
	Y₅	-20.0219	0.884043	0.166401	1.0326E-05	-6.6E-05	3.87E-05
	Y₆/100	1.011643	-0.005	-0.0005	3.10428E-06	6.1E-07	1.77E-05
	q	-15.3777	0.980967	0.025687	8.13625E-05	0.0001	-0.00018

	a₁	a₂	a₃	a₄	a₅	a₆
Y₁/1000	-0.07685	1.470297	-0.1705	-0.78328	2.137749	-2.20962
Y₂	31.2116	-68.1412	1.34441	39.5187	-3.5E-05	-0.29896
Y₃/1000	1.857377	0.03273	-1.61657	-9E-05	-2.22975	-0.06111
Y₄	13.15049	0.326402	1.135228	-0.00561	-4E-05	-9.9E-05
Y₅	38.22687	-86.4872	9.540386	12.56871	-0.12973	1.865674
Y₆/100	1.949455	0.04468	0.035642	-0.00084	-0.00011	-9.9E-05
Y₇/100	0.014616	0.005503	3.087246	1.06E-05	0.964806	-0.00829
Y₈	-1.66218	0.839116	-0.10119	-3.2E-06	-0.00747	2.849645
Y₉	0.002415	0.390498	0.863348	-0.00119	-2.3E-06	0.000429
Y₁₀/100	1.333315	-0.00324	-0.01079	2.32E-06	2.03E-05	3.39E-05
Y₁₁	-8.66117	-0.00972	1.120966	8.97E-05	1.58E-05	-0.00033
Y₁₂	-10.171	0.943874	0.047539	1.85E-05	0.000101	-7.8E-05
q	-2.76225	0.613628	0.382686	0.00257	0.002393	-0.00496

		Curing time	Data	R²	MAPE	RMSE	MAD
Group I	7 Day	Train	0.998	24.053	4.904	3.318	
		Test	0.999	25.133	5.013	3.500	
		Total	0.999	24.852	4.985	3.418	
	28 Day	Train	0.998	50.987	7.141	14.345	
		Test	0.997	52.111	7.219	15.092	
		Total	0.998	51.518	7.178	14.905	
	90 Day	Train	0.998	59.409	7.708	16.714	
		Test	0.994	60.893	7.803	17.635	
		Total	0.997	59.944	7.742	17.343	
Group II	Total	Train	0.999	50.534	7.109	14.033	
		Test	0.995	51.796	7.197	14.806	
		Total	0.998	50.989	7.141	14.560	

<i>q</i> , Model (stage)	R^2	<i>MAPE</i>	<i>RMSE</i>	<i>MAD</i>
<i>UCS Double hidden layer GMDH</i>	0.999	3.350	20.056	13.273
<i>UCS Three hidden layer GMDH</i>	0.999	3.212	20.488	12.731
<i>UCS MolaAbasi et al., [23]</i>	0.976	13.791	140.177	93.864
<i>UCS MolaAbasi and Shooshpasha [31]</i>	0.956	20.700	193.236	135.621
<i>UCS MolaAbasi and Shooshpasha [24]</i>	0.968	18.309	174.881	126.676